

## Sodalite: Spectroscopic and Thermochemical Investigations

Yu. D. Gritsenko<sup>a, b, \*</sup>, E. N. Eremina<sup>a, c</sup>, M. F. Vigasina<sup>a</sup>, S. V. Vyatkin<sup>a</sup>, L. P. Ogorodova<sup>b, \*\*</sup>,  
V. V. Maltsev<sup>a</sup>, and L. V. Melchakova<sup>a</sup>

<sup>a</sup> Geological Faculty, Lomonosov Moscow State University, Moscow, 119991 Russia

<sup>b</sup> Fersman Mineralogical Museum, Russian Academy of Sciences, Moscow, 119692 Russia

<sup>c</sup> Kola Science Centre, Laboratory of Arctic Mineralogy and Materials Science, Russian Academy of Sciences, Apatity, Murmansk region, 184209 Russia

\*e-mail: ygritsenko@rambler.ru

\*\*e-mail: logor48@mail.ru

Received October 20, 2022; revised November 8, 2022; accepted November 22, 2022

**Abstract**—Two sodalite samples (sample I is  $\text{Na}_8\text{Al}_6\text{Si}_6\text{O}_{24}\text{Cl}_2 \cdot 0.4\text{H}_2\text{O}$  from the Kovdor alkaline ultramafic massif with carbonatites in the Murmansk region, Russia, and sample II is  $\text{Na}_8\text{Al}_6\text{Si}_6\text{O}_{24}\text{Cl}_2 \cdot 0.2\text{H}_2\text{O}$  from the Bayan Kol nepheline syenite and miaskite massif in the Republic of Tyva) were studied by thermal and electron-microprobe analyses, powder X-ray diffraction, photoluminescence, and by IR, Raman, and ESR spectroscopy. Solution melt calorimetry was applied to determine the enthalpy of formation from elements for water-bearing sodalite samples:  $-13536 \pm 10$  (I) and  $-13503 \pm 19$  (II) kJ/mol. The enthalpy of formation of sodalite of the theoretical composition  $\text{Na}_8\text{Al}_6\text{Si}_6\text{O}_{24}\text{Cl}_2$  was evaluated at  $\Delta_f H^0(298.15 \text{ K}) = -13446 \pm 11$  kJ/mol. The data obtained on the enthalpy of formation of sodalite and literature data on its  $S^0(298.15 \text{ K})$  were used to calculate the standard Gibbs energies of formation of anhydrous and of water-bearing sodalite.

**Keywords:** X-ray powder diffraction, electron-microprobe analysis, photoluminescence, IR spectroscopy, ESR spectroscopy, Raman spectroscopy, thermal analysis, Calvet microcalorimetry, enthalpy, Gibbs energy, sodalite

**DOI:** 10.1134/S0016702923060046

### INTRODUCTION

Sodalite  $\text{Na}_8[\text{Al}_6\text{Si}_6\text{O}_{24}]\text{Cl}_2$  is a tectosilicate (framework silicate) whose structure consists of aluminosilicate cage network with fully ordered arrangement of Si, Al, and O atoms. The large interframework structure voids, so-called *sodalite lanterns*, are occupied by atoms, molecules, and ions connected with the framework by van der Waals or ionic bonds. Thanks to this structure, and similar to zeolites, sodalite is capable of ion-exchange reactions, which makes it valuable immobilizer filter used for deactivating radioactive wastes (Vance et al., 2014), including the  $^{129}\text{I}$  iodine isotope (Lin et al., 2022). As intraframework ions, sodalite can accommodate, by means of isomorphic exchange, potassium and calcium cations, hydroxyl, and sulfide and sulfate ions and thus form such sodalite-group minerals as hydrosodalite, hauyne, nosean, lazurite, and some others. The mineral belongs to the cubic crystallographic system, space group  $P\bar{4}3n$ .

Sodalite is a mineral that has been comprehensively studied by various physicochemical methods, such as X-ray powder diffraction and single-crystal X-ray diffraction (Peterson, 1983; Vance et al., 2014; Günther et al., 2015), IR absorption spectroscopy (Taylor et al.,

1971; Zilio and Bognato, 1984; Barnes et al., 1999; Günther et al., 2015; Škvarlova et al., 2019; Chukanov et al., 2020, 2022a, 2022b), Raman spectroscopy (Vance et al., 2014; Dumanska-Slowik et al., 2015; Günther et al., 2015; Škvarlova et al., 2019; Chukanov et al., 2020, 2022a, 2022b), ESR spectroscopy (McLaughlan and Marshall, 1970); Hodgson et al., 1967; Hassib et al., 1977; Annersten and Hassib, 1979; Pizani et al., 1985; Cano et al., 2010; Radomskaya et al., 2020), luminescence spectroscopy (Denisov et al., 1977; Tarashchan, 1978; Annersten and Hassib, 1979; Rogozhin et al., 1982; Cano et al., 2010, 2011; Dumanska-Slowik et al., 2015; Norrbo et al., 2015). Data on the thermal stability of the mineral are presented in (Antao and Hassan, 2002).

Sodalite is found mostly in magmatic rocks with medium and low silica concentrations, such as nepheline syenites, phonolites, and related rocks. The mineral is also formed by metasomatic processes in contact zones between limestones and/or marbles with nepheline syenite intrusions. Sodalite of magmatic origin (so-called *primary sodalite*) has been proved in experiments on NaCl dissolution in aluminosilicate melts (Kogarko, 1977) to be formed by the crystallization of Cl-rich magma. This element enriches the magma in the course of its crystallization and eventu-

ally induces its liquid immiscibility and the segregation of Cl-bearing portions from the residual aluminosilicate liquid, from which sodalite can then crystallize. Postmagmatic sodalite (so-called *secondary sodalite*) replaces nepheline, feldspar, and sometimes also aegirine. Sodalite-bearing mineral assemblages are formed within the temperature range of 500–900°C under a pressure of 3 kbar (Kotel'nikov et al., 1996).

The occurrence of sodalite in rocks is an important petrological indicator: the mineral contains much more Na than Al, and hence, the crystallization of this mineral is (along with the accommodation of alkalis in pyroxenes and amphiboles) is one of the principal indications of the origin of peralkaline mineralization (Borutskii, 1988).

When peralkaline rocks are studied, an important role is played by thermodynamic modeling of mineral-forming processes, which requires fundamental thermodynamic constants of sodalite and minerals in equilibrium with it (their enthalpy, Gibbs energy of formation, entropy, and heat capacity). One of the crucially important tasks of comprehensive physico-chemical studies of sodalite is to evaluate these constants. We are aware of only a single paper published so far on the calorimetric determination of the low-temperature heat capacity and enthalpy of formation of sodalite of the composition  $\text{Na}_8[\text{Al}_6\text{Si}_6\text{O}_{24}]\text{Cl}_2$  (Komada et al., 1995). Sharp et al. (1989) have estimated sodalite stability in the system  $\text{NaAlSi}_3\text{O}_8\text{--NaCl}$  and evaluated its Gibbs energy  $\Delta_f G^\circ(298.15 \text{ K})$ .

## EXPERIMENTAL

### *Samples*

This study was carried out with two sodalite samples from two massifs of different genetic type: sample I (no. 97731 in the collection of Fersman Mineralogical Museum (MMF), Russian Academy of Sciences, in Moscow) originated from the Kovdor ultramafic massif with carbonatites in the Murmansk region, Kola Peninsula, Russia; and sample II (MMF no. 97702) was taken from the Bayan Kol syenite and miaskite massif in the Republic of Tyva, southern central Siberia, Russia.

The Kovdor massif in the southwestern part of the Kola Peninsula is a complex multiphase ring intrusion, whose core consists of olivinite, and the peripheral zones are made up of alkaline rocks (ijolites and turiyaites). The youngest intrusive rocks of this massif are nepheline syenites, whose thin veins cut across the mafic rocks of the Kovdor massif: olivinites, ijolites, alkaline pyroxenites, etc. The nepheline syenites are massive coarse-grained gray rocks consisting mostly of feldspar, aegirine–diopside, and nepheline (the latter is usually variably replaced by cancrinite, zeolites, and other minerals). The principal accessory minerals are eudialyte, pectolite, sodalite, and vishnevite (Ivanyuk and Yakovenchuk, 1997).

The Bayan Kol nepheline syenite massif is located in the central part of the Sangilen Highland, 400 km south of the city of Kyzyl, the capital of the Republic of Tyva. The massif consists of feldspathic urtites (70–85% nepheline and 10–15% potassic feldspar), juvites, and nepheline syenites. These are leucocratic pale gray to greenish gray coarse-grained (up to giant-grained) massive rocks with clearly discernible nepheline crystals. Sodalite is found in this massif mostly in veins of nepheline syenite pegmatites (Andreeva et al., 1984).

Sample I was taken from a calcite–sodalite veinlet up to 0.5 cm thick hosted in a fine-grained phlogopite–pyroxene–nepheline rock at Zheleznyi Mine of the Kovdor deposit. The sodalite forms aggregates of colorless crystals up to 3 mm, which luminesce in pink in UV. The mineral shows photochromism, i.e., becomes pink when UV irradiated, with the color disappearing in daylight. Sample II is made up of a medium-grained aggregate of blue sodalite, which does not show visually detectable luminescence or photochromism, and occurs in association with potassic feldspar, albite, and phlogopite.

### *Methods*

The **chemical composition** of the samples was analyzed on a JSM-6480LV (Jeol Ltd., Japan) scanning electron microscope with a tungsten cathode, equipped with an X-Max-50 (Oxford Instruments Ltd., Great Britain) energy-dispersive spectrometer at an accelerating voltage of 20 kV and beam current of  $10.05 \pm 0.05 \text{ nA}$ . The raw spectra were processed with the INCA (Oxford Instruments, v. 22) software.

The **thermogravimetric analysis** was carried out to determine water, on a NETZSCH STA 449F5 (Germany) system for thermal analysis within the temperature range from room temperature to 973 K, at a heating rate of 10 K/min in an argon atmosphere. The masses of samples I and II were 45 and 54 g, respectively. The instrument was calibrated on proprietary standards provided by the manufacturer.

The **X-ray diffraction study** was conducted on an ADP-2 (Russia) X-ray powder diffractometer, using Co radiation and a Fe filter. The operation parameters were as follows: 35 kV, 25 Ma, and  $0.02^\circ$  angle increments.

The **Raman spectroscopic study** was carried out on an EnSpectr R532 (Russia) Raman microscope within the range of 100–4000  $\text{cm}^{-1}$  and a spectral resolution of approximately 6  $\text{cm}^{-1}$ . The wavelength of the exciting laser radiation was 532 nm, and the output power was 9 mW. The holographic dispersion grating had 1800 grooves/mm, and the focal spot at  $40\times$  magnification was 10  $\mu\text{m}$  in diameter. The spectra were obtained from randomly oriented samples, by averaging over 100 exposures. The standard for the calibration of the instrument was a silicon platelet (scattering line at 521  $\text{cm}^{-1}$ ).

The **IR spectroscopic study** was conducted on a FSM-1201 (Russia) Fourier spectrometer in transmission mode, in air, at room temperature, within the range of wavenumbers of 400 to 4000  $\text{cm}^{-1}$ , with the signal averaged over 15 scans at a resolution of 4  $\text{cm}^{-1}$ . The samples were prepared in the form of suspension of 4–5 mg of the mineral powder in paraffinic oil. The suspension was applied to a KBr platelet, which had been used as the reference sample before the mineral suspension was applied to it.

The **photoluminescence study** of the sodalite was conducted on a LOT-Oriel MS–257 (United States) spectrograph at room temperature. The excitation source of the UV radiation was a Xe lamp (150 W), the radiation was within the range of 200–900 nm.

The **ESR study** was done on a Varian E-115 (United States–Switzerland) ESR spectrometer at the X band (~9.4 GHz) at a modulation amplitude of 0.1 mTesla at a modulation frequency of 100 kHz and microwave radiation power of 0.2 mW, using single-crystal samples in the orientation  $H||L_4$ .

The **thermochemical study** of the sodalite was carried out using a SETARAM Tian–Calvet (France) high-temperature conducting microcalorimeter, by dissolving in melt of the composition  $2\text{PbO}\cdot\text{B}_2\text{O}_3$ , which had been obtained by fusing stoichiometric amounts of lead oxide and boracic acid at 1073 K. The melt-solution experiments were done in air by dropping crystals 2–8 ( $\pm 2 \times 10^{-3}$ ) mg in mass from room temperature into melt in a calorimeter at  $T = 973$  K. The measured heat change consisted of the change in the enthalpy of the sample [ $H^0(973 \text{ K}) - H^0(298.15 \text{ K})$ ] and its dissolution enthalpy  $\Delta_{\text{dissol}}H^0(973 \text{ K})$ . At six to eight experiments with the same melt portion (30–35 g), the mass ratio of the dissolved matter to the solvent could be regarded as infinitely diluted solution of negligibly small mixing enthalpy. The instrument was calibrated by measuring the change in the enthalpy of a standard reference material (platinum) at the parameters of the dissolution experiments. The required data on [ $H^0(973 \text{ K}) - H^0(298.15 \text{ K})$ ] of Pt were compiled from (Robie and Hemingway, 1995).

The ADP-2 scanning X-ray powder diffractometer, JSM-6480LV scanning electron microscope, FSM-1201 IR Fourier spectrometer, EnSpectr R532 Raman microscope, NETZSCH STA 449F5 thermal system, Varian E-115 ESR spectrometer, and Setaram Tian–Calvet microcalorimeter used in this study are installed at the Geological faculty of Lomonosov Moscow State University; and the LOT-Oriel MS–257 spectrograph is installed at the Chemical Faculty of the same University.

## RESULTS

The **chemical composition** of the sodalite is presented in Table 1 based on microprobe (EPMA) data.

**Table 1.** Chemical composition (wt %) of the sodalite samples

Component	Sample I <sup>a</sup>	Sample II <sup>b</sup>	Sample III <sup>c</sup>
Na <sub>2</sub> O	24.97	24.99	25.70
K <sub>2</sub> O	n.d.	0.01	0.04
CaO	n.d.	n.d.	n.d.
FeO	n.d.	n.d.	0.01
Al <sub>2</sub> O <sub>3</sub>	31.52	31.46	31.20
SiO <sub>2</sub>	36.60	36.59	35.98
S <sub>tot.</sub>	n.d.	n.d.	0.37
Cl	7.40	7.32	7.30
H <sub>2</sub> O <sup>d</sup>	0.73	0.40	n.a.
Total	101.22	100.76	100.60

<sup>a</sup> Average of four measurements.

<sup>b</sup> Average of five measurements.

<sup>c</sup> Average of three determinations, the sample was used to compare the ESR spectroscopic results.

<sup>d</sup> According to thermogravimetric data.

The water content was determined from data of thermogravimetric analysis. Both the TG and the DTG curves indicate a mass loss of the sample within the temperature range of ~100–700°C, which means the absence of adsorption water and the presence of water in the structural voids (so-called *sodalite lanterns*). The sodalite formulas normalized to 50 changes are  $\text{Na}_{7.95}[\text{Al}_{6.07}\text{Si}_{5.97}\text{O}_{24}]\text{Cl}_{2.04}\cdot 0.40\text{H}_2\text{O}$  (for sample I) and  $\text{Na}_{7.92}[\text{Al}_{6.06}\text{Si}_{5.98}\text{O}_{24}]\text{Cl}_{2.02}\cdot 0.22\text{H}_2\text{O}$  (for sample II). Both are similar to each other and to the theoretical formula of sodalite  $\text{Na}_8\text{Al}_6\text{Si}_6\text{O}_{24}\text{Cl}_2$ .

The **X-ray diffraction spectra** of the sodalite samples correspond to the sodalite spectra in the databases ICDD (The International Centre for Diffraction Data, 2013; card no. 01-075-0709), RRUFF (Database of Raman Spectroscopy, X-Ray Diffraction and Chemistry of Minerals; card no. R060436), and MINCRYST (Crystallographic and Crystal-Chemical Database for Minerals and Their Structural Analogues, card no. 4415). The calculated unit-cell parameters of the cubic unit cell are  $a = 8.86909 \text{ \AA}$  (sample I) and  $8.86692 \text{ \AA}$  (sample II) and are close to the value  $a = 8.8690 \text{ \AA}$  for the sample in the electronic database MINCRYST (Crystallographic and Crystal-Chemical Database for Minerals and Their Structural Analogues, card no. 4415).

The **Raman spectra** obtained in the course of this study (Fig. 1) are consistent with those of sodalite samples from Canada and Afghanistan in the database RRUFF (Database of Raman spectroscopy, X-ray Diffraction and Chemistry of Minerals, card nos. R040141, R060354/355, R060416, and R060435/436). The spectral lines were identified according to (Hettmann et al., 2012): the line with a maximum at 1062/1065  $\text{cm}^{-1}$  (here and below, the values in the

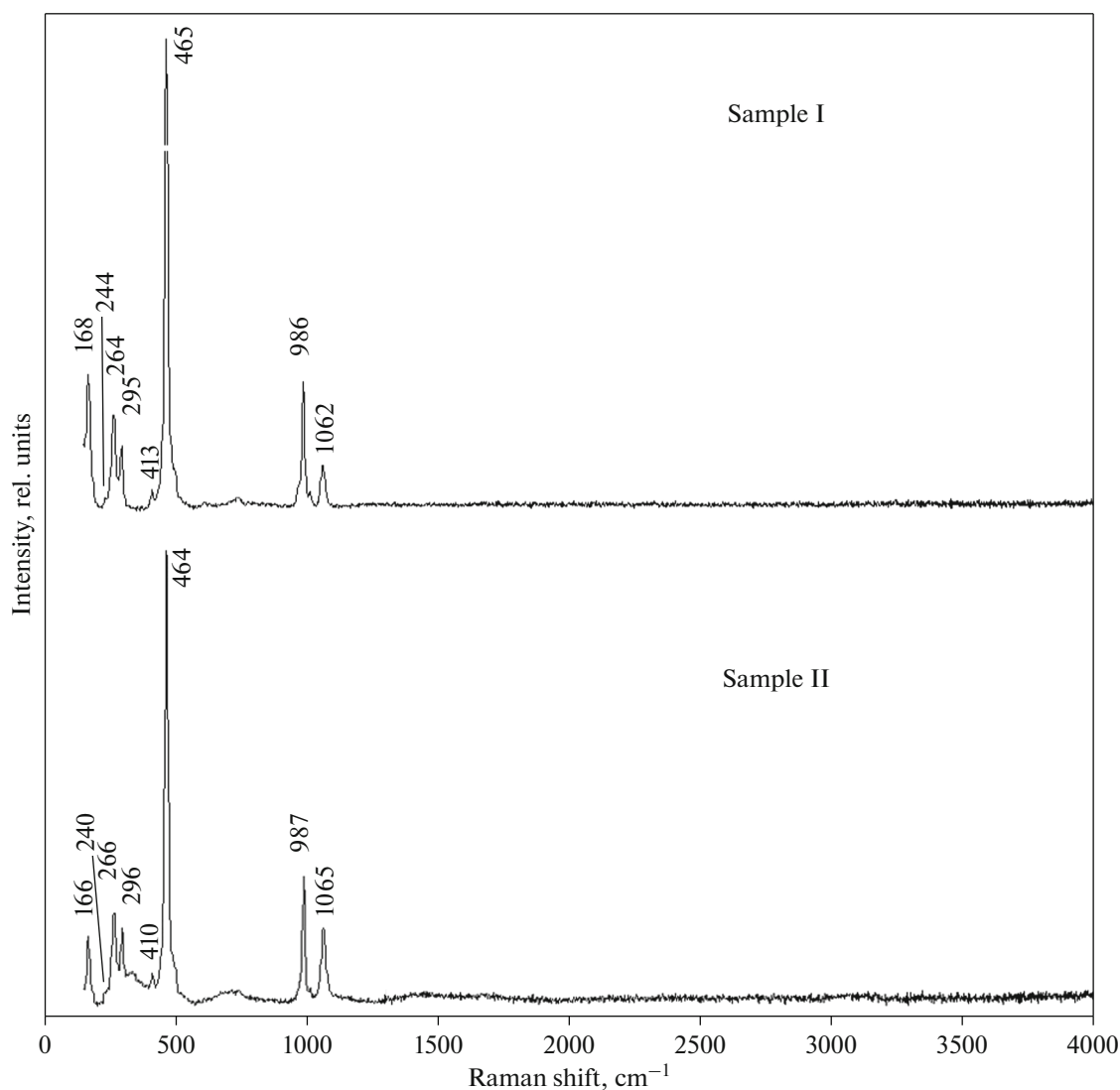


Fig. 1. Raman spectra of the sodalite samples.

numerator and denominator refer to samples I and II, respectively) reportedly corresponds to the antisymmetric valence oscillations of  $(\text{Al},\text{Si})\text{O}_4$  the tetrahedrons, and the more intense line with a maximum at  $986/987\text{ cm}^{-1}$  corresponds to the symmetric valence oscillations of these tetrahedrons. The low-intensity line with a maximum at  $616/619\text{ cm}^{-1}$  is assigned to the valence oscillations of the  $(\text{Al},\text{Si})\text{O}_4$  tetrahedrons and Al–O and Si–O bonds; the most intense line in the spectrum at  $465/464\text{ cm}^{-1}$  is caused by the valence oscillations of  $\text{ClNa}_4$  tetrahedrons; the low-intensity line with a maximum at  $413/410\text{ cm}^{-1}$  and the line at approximately  $295/296\text{ cm}^{-1}$  reportedly correspond to the deformation oscillations of  $(\text{Al},\text{Si})\text{O}_4$  tetrahedrons; the nearby line with a maximum at  $264/266\text{ cm}^{-1}$  corresponds to the deformation oscillations of these tetrahedrons and valence oscillations of Na–O bonds; the very low-intensity line with a frequency of about

$244/240\text{ cm}^{-1}$  is thought to be caused by the deformation oscillations of  $\text{ClNa}_4$  tetrahedrons; and the medium-intensity line at  $168/166\text{ cm}^{-1}$  corresponds to lattice modes.

The **IR absorption spectra** of the samples (Fig. 2) are compatible with the spectra of sodalite from northern Karelia, Russia, published in (Chukanov, 2014; sample Sif21); the wavenumbers of the absorption bands in the spectra of these samples coincide within  $2\text{--}3\text{ cm}^{-1}$ . The wide intense bands with absorption maxima at  $980/978\text{ cm}^{-1}$  and a shoulder at  $1026\text{ cm}^{-1}$  may be attributed to the antisymmetric valence oscillations of Si–O and Al–O bonds in the aluminosilicate framework. The spectral region of  $600\text{ to }750\text{ cm}^{-1}$  includes complex bands, which consist of three components with the deformation oscillations of the O–Al–O and O–Si–O angles; the absorption bands consisting of two components with maxima at  $467/467$  and

436/435  $\text{cm}^{-1}$  correspond to so-called lattice oscillation modes. In the high-frequency spectral region, very low-intensity absorption bands were registered that correspond to the valence oscillations of OH groups.

The fact that the spectrum of sample II involves an additional low-intensity absorption band with a maximum at 580  $\text{cm}^{-1}$ , which is absent from the spectrum of sample I, indicates (Prokof'ev and Gordina, 2014) that the structure of sample II includes zeolite fragments: *D4R* double-four-rings (Fig. 3), and the band corresponds to the valence oscillations of these rings. It has been demonstrated in the aforementioned publications that double-four-rings characteristic of zeolite structures are formed at lower alkalinity of the crystallization medium (NaOH concentration of 2–4 mol/L), and only *S4R* single-four-rings can be formed at higher alkalinity ( $\geq 8$  mol/L) (Fig. 3), which are typical of the sodalite structure. Based on these results in the aforementioned paper, it is reasonable to hypothesize that the sodalite from Tyva (sample II) crystallized at lower alkalinity than that of the sodalite from Kovdor (sample I).

**Photoluminescence spectroscopy.** Figure 4 show the luminescence spectrum of the sodalite (sample I) with a radiation maximum at 680–690 nm, which indicates that the sample contains  $\text{S}_2^-$  radicals, which are responsible for the luminescence in the orange–red spectral region at UV excitation (Tarashchan et al., 1970; Tarashchan, 1978). The absence of sulfur from this sample is explained by its concentration below the EPMA detection limit. Sample II did not exhibit luminescence at UV excitation.

**ESR study.** The spectra of samples I and II (Fig. 5) in the orientation  $H \parallel L_4$  involved registered anisotropic signals with the factors  $g = 2.049$  and  $2.004$ , which differed from each other only by the ratios of the intensities and did not correlate with the colors of the samples. If the geometry of the experiments was changed ( $H$  not parallel to  $L_4$ ), the intensities of both lines significantly decreased. A signal with an effective  $g = 2.049$  was transformed into a triplet (in the general position) upon the change in the orientation, whereas the signal with  $g = 2.004$  remained singlet. Inasmuch as the lines occur in the spectra of the single-crystal specimens regardless of their color, and with regard to the fact that the signals are anisotropic, it is reasonable to suggest that they correspond to signals obtained from the powdered samples in (Hodgson et al., 1967). The signal with a factor  $g = 2.016$  was attributed by these authors to the paramagnetic center  $\text{S}_2^-$ , and the signal with  $g = 2.006$  was provisionally ascribed to the defect on oxygen.

In addition, the spectrum of sample II (blue sodalite) involved an intense anisotropic signal (Fig. 5) with  $g = 2.012$ , which is close to the values obtained in (Annersten and Hassib, 1979; Pizani et al., 1985):

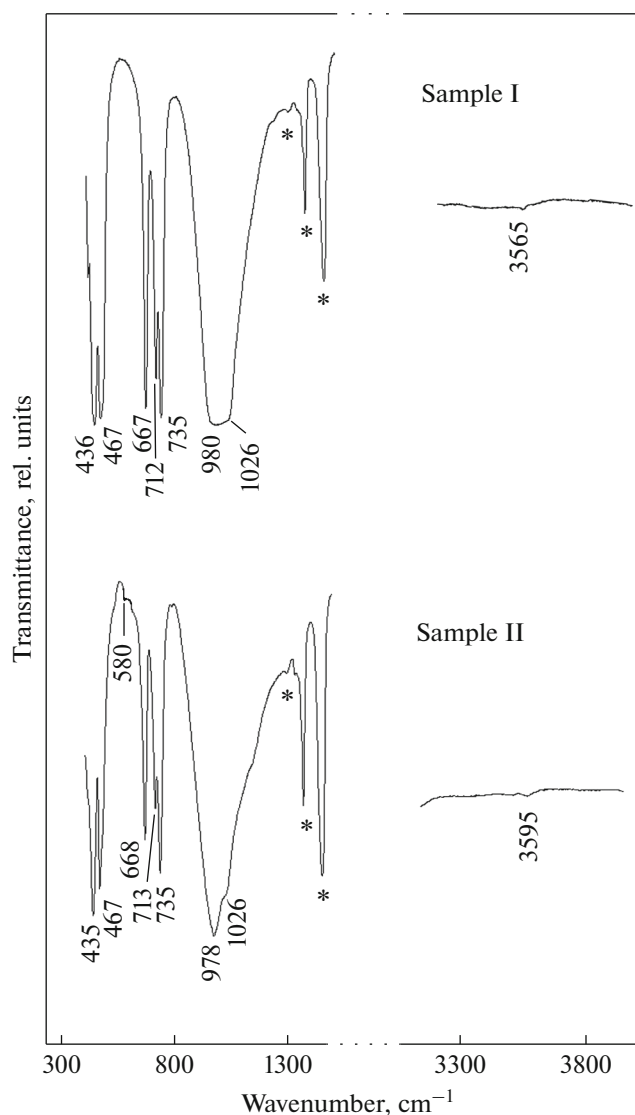


Fig. 2. IR absorption spectra of the sodalite samples (recorded in transmittance mode, \* is the absorption bands of paraffinic oil).

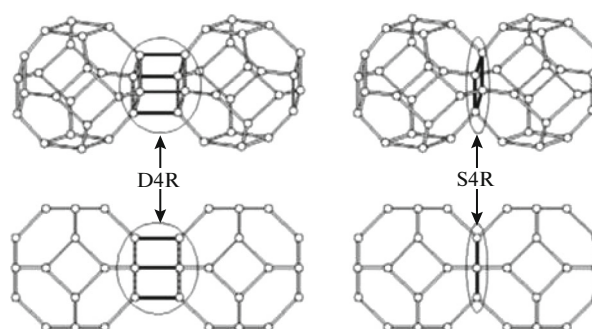


Fig. 3. *D4R* double-four-ring typical of the zeolite structure and a *S4R* single-four-ring characteristic of the sodalite structure (Prokof'ev and Gordina, 2014).

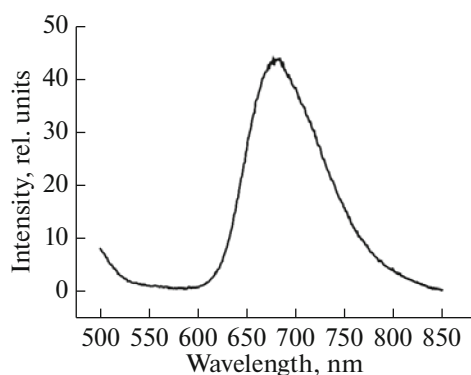


Fig. 4. Photoluminescence spectrum of the sodalite (sample I).

$g = 2.0112$  and  $g = 2.011$ , respectively. Annersten and Hassib (1979) believed that this signal of the ESR spectrum and the line at 580 nm, which they registered in the visible region of the absorption spectrum and which is responsible for the blue color of the mineral, are related to the presence of colloid particles of metallic Na. However, this explanation was questioned in (Pizani et al., 1985), in which this ESR signal was explained as related to interstitial oxygen.

Hodgson et al. (1967) detected a correlation between the intensity of the pink color of sodalite and the intensities of the thirteen equally spaced ESR lines ( $g = 2.002$ , 30.6 G apart centered), which result from the interaction of an electron entrapped at a Cl vacancy with four Na nuclei surrounding this vacancy. The theoretical ratios of the intensities of lines for such a center is 1 : 4 : 10 : 20 : 31 : 40 : 44 : 40 : 31 : 20 : 10 : 4 : 1. These authors observed such multiline spectra obtained from all sodalite samples with photochromism. However, no such a signal was identified in our

ESR spectrum from sample I (which displayed photochromism). In view of this, we have studied a sodalite sample from the Malaya Bystraya deposit in the Slyudyanka district, Irkutsk region, southern central Siberia (sample III), which also showed orange-red luminescence but was richer in sulfur (see Table 1 for the chemical analysis) and showed a much stronger photochromic effect.

Sample III was studied with regard to the results in (Hodgson et al., 1967), in which the authors applied UV irradiation immediately in the resonance chamber of the ESR spectrometer. In our experiment, UV irradiation (254 nm) was carried out for 0.5 h before the ESR measurements. This allowed us to record only the central, the most intense part of the multiline signal (Fig. 5). Our parameters of the signal ( $g = 2.002$ , 30.5 G apart centered) well correlate with the results of the aforementioned publication, whose authors believed that the photochromic effect is caused by the occurrence of  $S_2^{2-}$  ions in the sodalite structure, which are thought to be the source of the electrons temporarily captured by the Cl ion vacancies under the effect of UV radiation, at the origin of the  $F$  centers. Hence, the occurrence of sulfur in sample III in the form of  $S_2^-$  has been confirmed by typical luminescence and is consistent with the scenario proposed in (Hodgson et al., 1967) for the origin of paramagnetic centers responsible for the photochromic effect of sodalite. Our results suggest that the photochromic effect of sample I may have been formed by an analogous mechanism.

**Enthalpy of formation from elements.** The thermodynamic constants were calculated for simplified formulas of our samples and for the theoretical formula of sodalite. The following values were obtained:  $[H^0(973\text{ K}) - H^0(298.15\text{ K}) + \Delta_{\text{dissol}}H^0(973\text{ K})]$ :  $1267 \pm 6\text{ J/g} = 1237 \pm 6\text{ kJ/mol}$  ( $M = 976.43\text{ g/mol}$ ) for sam-

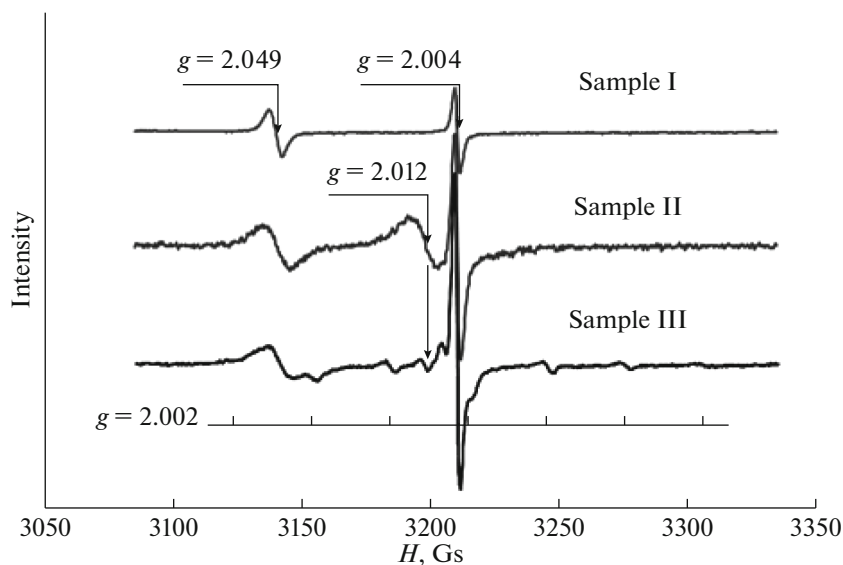


Fig. 5. ESR spectra of the sodalite samples recorded in orientation  $H \parallel L_4$ .

**Table 2.** Thermochemical data used to calculate the enthalpy of formation (kJ/mol) of sodalite

Component	$H^0(973\text{ K}) - H^0(298.15\text{ K}) + \Delta_{\text{dissol}}H^0(973\text{ K})$	$-\Delta_f H^0(298.15\text{ K})^a$
Na <sub>2</sub> O(cr)	$-111.8 \pm 0.8^b$	$414.8 \pm 0.3$
Al <sub>2</sub> O <sub>3</sub> (corundum)	$107.38 \pm 0.59^c$	$1675.7 \pm 1.3$
SiO <sub>2</sub> (quartz)	$39.43 \pm 0.21^d$	$910.7 \pm 1.0$
NaCl(halite)	$65.19 \pm 1.42^e$	$411.3 \pm 0.1$
Al(OH) <sub>3</sub> (gibbsite)	$172.6 \pm 1.9^f$	$1293.1 \pm 1.2$

<sup>a</sup> Published tabulated data (Robie and Hemingway, 1995).

<sup>b</sup> According to data in (Kiseleva et al., 2001).

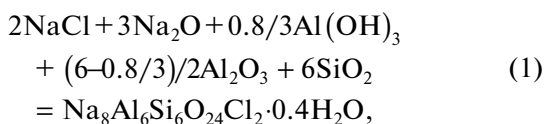
<sup>c-e</sup> Calculated using published tabulated data on  $[H^0(973\text{ K}) - H^0(298.15\text{ K})]$  (Robie and Hemingway, 1995) and experimental data on dissolution  $\Delta_{\text{dissol}}H^0(973\text{ K})$ : <sup>c</sup> (Ogorodova et al., 2003), <sup>d</sup> (Kiseleva et al., 1979), <sup>e</sup> (Kiseleva et al., 1990).

<sup>f</sup> According to data in (Ogorodova et al., 2011).

ple I of the composition Na<sub>8</sub>Al<sub>6</sub>Si<sub>6</sub>O<sub>24</sub>Cl<sub>2</sub>·0.4H<sub>2</sub>O (average of the results of eight measurements) and  $1294 \pm 17\text{ J/g} = 1259 \pm 17\text{ kJ/mol}$  ( $M = 972.82\text{ g/mol}$ ) for sample II of the composition Na<sub>8</sub>Al<sub>6</sub>Si<sub>6</sub>O<sub>24</sub>Cl<sub>2</sub>·0.2H<sub>2</sub>O (average of the results of nine measurements); the errors were calculated at 95% probability.

The calorimetric data obtained for the sodalite samples and the thermochemical cycle, which involved the dissolution of the mineral and its components, were used to calculate the enthalpy of formation of sodalite with various amounts of zeolite-type water.

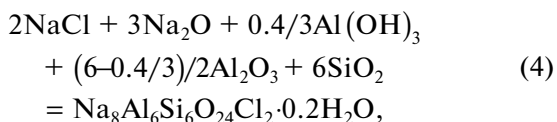
For sample I



$$\Delta_{r(1)}H^0(298.15\text{ K}) = 2\Delta_f H^0\text{NaCl} + 3\Delta_f H^0\text{Na}_2\text{O} + 0.8/3\Delta_f H^0\text{Al}(\text{OH})_3 + (6-0.8/3)/2\Delta_f H^0\text{Al}_2\text{O}_3 + 6\Delta_f H^0\text{SiO}_2 - \Delta_f H^0\text{Na}_8\text{Al}_6\text{Si}_6\text{O}_{24}\text{Cl}_2 \cdot 0.4\text{H}_2\text{O}, \quad (2)$$

$$\Delta_f H^0(298.15\text{ K})\text{Na}_8\text{Al}_6\text{Si}_6\text{O}_{24}\text{Cl}_2 \cdot 0.4\text{H}_2\text{O} = \Delta_{r(1)}H^0(298.15\text{ K}) + 2\Delta_f H^0(298.15\text{ K})\text{NaCl} + 3\Delta_f H^0(298.15\text{ K})\text{Na}_2\text{O} + 0.8/3\Delta_f H^0(298.15\text{ K})\text{Al}(\text{OH})_3 + (6-0.8/3)/2\Delta_f H^0(298.15\text{ K})\text{Al}_2\text{O}_3 + 6\Delta_f H^0(298.15\text{ K})\text{SiO}_2, \quad (3)$$

and for sample II

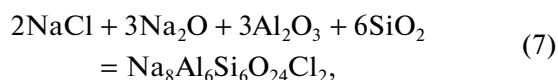


$$\Delta_{r(4)}H^0(298.15\text{ K}) = 2\Delta_f H^0\text{NaCl} + 3\Delta_f H^0\text{Na}_2\text{O} + 0.4/3\Delta_f H^0\text{Al}(\text{OH})_3 + (6-0.4/3)/2\Delta_f H^0\text{Al}_2\text{O}_3 + 6\Delta_f H^0\text{SiO}_2 - \Delta_f H^0\text{Na}_8\text{Al}_6\text{Si}_6\text{O}_{24}\text{Cl}_2 \cdot 0.2\text{H}_2\text{O}, \quad (5)$$

$$\begin{aligned} & \Delta_f H^0(298.15\text{ K})\text{Na}_8\text{Al}_6\text{Si}_6\text{O}_{24}\text{Cl}_2 \cdot 0.2\text{H}_2\text{O} \\ &= \Delta_{r(1)}H^0(298.15\text{ K}) + 2\Delta_f H^0(298.15\text{ K})\text{NaCl} \\ & \quad + 3\Delta_f H^0(298.15\text{ K})\text{Na}_2\text{O} \\ & \quad + 0.4/3\Delta_f H^0(298.15\text{ K})\text{Al}(\text{OH})_3 \\ & \quad + (6-0.4/3)/2\Delta_f H^0(298.15\text{ K})\text{Al}_2\text{O}_3 \\ & \quad + 6\Delta_f H^0(298.15\text{ K})\text{SiO}_2, \end{aligned} \quad (6)$$

where  $\Delta H = [H^0(973\text{ K}) - H^0(298.15\text{ K}) + \Delta_{\text{dissol}}H^0(973\text{ K})]$  is thermochemical data for the sodalite samples and for Na, Al, and Si oxides, Na chloride, and Al hydroxide (Table 2) the needed values to calculate the values of  $\Delta_f H^0(298.15\text{ K})$  for the components of this reaction are presented in (Table 2). The calculated enthalpy values of the formation of the sodalite samples are listed in Table 3.

Our experimental data on the dissolution of the sodalite samples were used to calculate the enthalpy of formation of sodalite of the theoretical composition Na<sub>8</sub>Al<sub>6</sub>Si<sub>6</sub>O<sub>24</sub>Cl<sub>2</sub>. To do this, we recalculated the data of the calorimetric experiments onto its molecular weight ( $M = 969.22\text{ g/mol}$ ) and used in calculations by reaction (7) and equations (8) and (9)



$$\Delta_{r(7)}H^0(298.15\text{ K}) = 2\Delta_f H^0\text{NaCl} + 3\Delta_f H^0\text{Na}_2\text{O} + 3\Delta_f H^0\text{Al}_2\text{O}_3 + 6\Delta_f H^0\text{SiO}_2 - \Delta_f H^0\text{Na}_8\text{Al}_6\text{Si}_6\text{O}_{24}\text{Cl}_2, \quad (8)$$

$$\begin{aligned} & \Delta_f H^0(298.15\text{ K})\text{Na}_8\text{Al}_6\text{Si}_6\text{O}_{24}\text{Cl}_2 \\ &= \Delta_{r(7)}H^0(298.15\text{ K}) \\ & \quad + 2\Delta_f H^0(298.15\text{ K})\text{NaCl} \\ & \quad + 3\Delta_f H^0(298.15\text{ K})\text{Na}_2\text{O} \\ & \quad + 3\Delta_f H^0(298.15\text{ K})\text{Al}_2\text{O}_3 + 6\Delta_f H^0(298.15\text{ K})\text{SiO}_2. \end{aligned} \quad (9)$$

The required thermochemical data for the compounds involved in reaction (7) were compiled from Table 2. The calculated values of the enthalpy of formation of sodalite of theoretical composition from



**Table 3.** Thermodynamic properties of sodalite obtained in this study

Sodalite composition and its molecular weight, g/mol	$-\Delta_f H^0(298.15 \text{ K})^a$ , kJ/mol	$S^0(298.15 \text{ K})^b$ , J/(mol K)	$-\Delta_f S^0(298.15 \text{ K})^c$ , L/(mol K)	$-\Delta_f G^0(298.15 \text{ K})^d$ , kJ/mol
$\text{Na}_8\text{Al}_6\text{Si}_6\text{O}_{24}\text{Cl}_2 \cdot 0.4\text{H}_2\text{O}$ $M = 976.43$	$13536 \pm 10$	$864 \pm 4$	$2515 \pm 4$	$12786 \pm 10$
$\text{Na}_8\text{Al}_6\text{Si}_6\text{O}_{24}\text{Cl}_2 \cdot 0.2\text{H}_2\text{O}$ $M = 972.82$	$13503 \pm 19$	$856 \pm 4$	$2523 \pm 4$	$12751 \pm 19$
$\text{Na}_8\text{Al}_6\text{Si}_6\text{O}_{24}\text{Cl}_2$ $M = 969.22$	$13446 \pm 11$	$848 \pm 4$	$2531 \pm 4$	$12691 \pm 11$

<sup>a</sup> Data of melt solution calorimetry.

<sup>b</sup> Data in (Komada et al., 1995).

<sup>c</sup> Calculated using data on  $S^0(298.15 \text{ K})$  for elements composing sodalite (Robie and Hemingway, 1995).

<sup>d</sup> Calculated by the formula  $\Delta_f G^0 = \Delta_f H^0 - T\Delta_f S^0$ .

elements ( $-13\,433 \pm 10$  and  $-13\,459 \pm 19$  kJ/mol, calculated using calorimetric data on sodalite samples I and II, respectively), are consistent, within the errors, with one another and with data in (Komada et al., 1995). In this publication, the value of  $\Delta_f H^0(298.15 \text{ K}) = -13457.0 \pm 15.8$  kJ/mol was also obtained by high-temperature melt solution calorimetry for a sodalite sample from Mount St. Hilaire, Quebec, Canada, based on a thermochemical cycle involving compounds different from those we used for the calculations. The consistency of the data confirms their reliability and verifies them. The average of our values of  $\Delta_f H^0(298.15 \text{ K})$  is presented in Table 3.

**Gibbs energy of formation from elements.** The value of  $\Delta_f G^0(298.15 \text{ K})$  of sodalite of theoretical composition (Table 3) was calculated using the enthalpy value obtained above and literature data on the standard entropy determined in (Komada et al., 1995) based on the low-temperature heat capacity of a natural sample measured within the temperature range of 15–350 K. The calculated Gibbs energy value of sodalite ( $-12\,691 \pm 11$  kJ/mol) is consistent with the estimates (presented without specified errors) in (Sharp et al., 1989):  $\Delta_f G^0(298.15 \text{ K}) = -12\,697$  kJ/mol. The Gibbs free energy of formation from elements of natural water-bearing sodalite samples (Table 3) were calculated with the use of the values of  $S^0(298.15 \text{ K})$  based on data in (Komada et al., 1995), with regard to the entropy contributions corresponding to the water concentrations in the samples according to (Naumov et al., 1971).

## CONCLUSIONS

The photochromism effect of sodalite seems to be indicative of that the mineral contains  $F$  centers, and hence, sulfur in the form of the  $S_2^-$  radical. The photochromic effect is visually discernible even at extremely low concentrations of sulfur and  $F$  centers in the sample, which cannot be identified even by using high-precision laboratory techniques.

The fundamental thermodynamic properties of anhydrous and water-bearing sodalite calculated in

this study can be recommended for entering into databases of thermodynamic constants of minerals and can be utilized in modeling mineral-forming processes in magmatic agpaitic alkaline and metasomatic rocks.

## CONFLICT OF INTEREST

The authors declare that they have no conflicts of interest.

## REFERENCES

- E. D. Andreeva, V. A. Kononova, E. V. Sveshnikova, and R. M. Yashina, *Igneous Rocks. Volume 2. Alkaline Rocks* (Nauka, Moscow, 1984) [in Russian].
- H. Annersten and A. Hassib, "Blue sodalite," *Can. Mineral.* **17**, 39–46 (1979).
- S. Antao and I. Hassan, "Thermal analyses of sodalite, tugtupite, danalite and helvite," *Can. Mineral.* **40**, 163–172 (2002).
- M. C. Barnes, J. Addai-Mensah, and A. R. Gerson, "A methodology for quantifying sodalite and cancrinite phase mixtures and the kinetics of the sodalite to cancrinite phase transformation," *Micropor. Mesopor. Mater.* **31**, 303–319 (1999).
- B. E. Borutskii, *Rock-Forming Minerals of High-Alkali Complexes* (Nauka, Moscow, 1988) [in Russian].
- N. F. Cano, A. R. Blak, and S. Watanabe, "Correlation between electron paramagnetic resonance and thermoluminescence in natural sodalite," *Phys. Chem. Miner.* **37**, 57–64 (2010).
- N. F. Cano, A. R. Blak, J. S. Ayala-Arenas, and S. Watanabe, "Mechanisms of TL for production of the 230°C peak in natural sodalite," *J. Lumin.* **131**, 165–168 (2011).
- N. V. Chukanov, M. F. Vigasina, N. V. Zubkova, I. V. Pekov, C. Schäfer, A. V. Kasatkin, V. O. Yapaskurt, and D. Yu. Pushcharovsky, "Extra-framework content in sodalite–group minerals: complexity and new aspects of its study using infrared and Raman spectroscopy," *Mineralogy* **10**, # 363 (2020).
- N. V. Chukanov, R. Yu. Shendrik, M. F. Vigasina, I. V. Pekov, A. N. Sapozhnikov, V. D. Shcherbakov, and D. A. Varlamov, "Crystal chemistry, isomorphism, and thermal conversions of extra-framework components in sodalite–group minerals," *Minerals* **12**, # 887 (2022a).
- N. V. Chukanov, N. V. Zubkova, I. V. Pekov, R. Yu. Shendrik, D. A. Varlamov, M. F. Vigasina, D. I. Belakovskiy,



- S. N. Britvin, V. O. Yapaskurt, and D. Yu. Pushcharovsky, "Sapozhnikovite,  $\text{Na}_8(\text{Al}_6\text{Si}_6\text{O}_{24})(\text{HS})_2$ , a new sodalite-group mineral from the Lovozero alkaline massif, Kola Peninsula," *Mineral. Mag.* **86**, 49–59 (2022b).
- R. A. Denisov, V. P. Denks, A. E. Dudelzak, V. S. Osminin, and T. V. Ruus, "Optically erasable coloration and luminescence of sodalites," *Zh. Phys. Chem.* **27** (1), 149–154 (1977).
- M. Dumańska-Słowik, W. Heflik, A. Pieczka, and M. Sikorska, "The transformation of nepheline and albite into sodalite in pegmatitic mariupolite of Oktiabrski Massif (SE Ukraine)," *Spectrachim. Acta. Part A: Mol. Biomol. Spectr.* **150**, 837–845 (2015).
- C. Günther, H. Richter, I. Voigt, A. Michaelis, H. Tzscheuschler, R. Krause-Rehberg, and J. M. Serra, "Synthesis and characterization of a sulfur containing hydroxyl sodalite without sulfur radicals," *Micropor. Mesopor. Mater.* **214**, 1–7 (2015).
- A. Hassib, O. Beckman, and H. Annersten, "Photochromic properties of natural sodalite," *J. Phys. D: Appl. Phys.* **10**, 771–777 (1977).
- K. Hettmann, T. Wenzel, M. Marks, and G. Markl, "The sulfur speciation in S-bearing minerals: New constraints by combination of electron microprobe analysis and DFT calculations with special reference to sodalite-group minerals," *Am Mineral.* **97**, 1653–1661 (2012).
- W. G. Hodgson, J. S. Brinen, and E. F. Williams, "Electron spin resonance investigation of photochromic sodalities," *J. Chem. Physics.* **47** (10), 3719–3723 (1967).
- G. Yu. Ivanyuk and V. N. Yakovenchuk, *Minerals of Kovdor* (Kolskii NTs RAN, Apatity, 1997) [in Russian].
- I. A. Kiseleva, L. P. Ogorodova, N. D. Topor, and O. G. Chigareva, "Thermochemical study of the  $\text{CaO-MgO-SiO}_2$  system," *Geokhimiya*, no. 12, 1811–1825 (1979).
- I. A. Kiseleva, L. P. Ogorodova, Yu. I. Sidorov, and I. L. Khodakovskii, "Thermodynamic properties of alkaline feldspars," *Geokhimiya*, No. 3, 406–413 (1990).
- I. A. Kiseleva, A. Navrotsky, I. A. Belitsky, and B. A. Fursenko, "Thermochemical study of calcium zeolites—heulandite and stilbite," *Am. Mineral.* **86**, 448–455 (2001).
- L. N. Kogarko, *Problems of Genesis of Agpaitic Magmas* (Nauka, Moscow, 1977) [in Russian].
- N. Komada, E. F. Westrum, B. S. Hemingway, M. Yu. Zolotov, Yu. V. Semenov, I. L. Khodakovskiy, and L. M. Anovitz, "Thermodynamic properties of sodalite at temperatures from 15 K to 1000 K," *J. Chem. Thermodynam.* **27**, 1119–1132 (1995).
- A. R. Kotelnikov, L. V. Zhorniyak, and Z. A. Kotel'nikova, "Distribution of sulfur between sodalite and hydrothermal fluid: an experimental study," *Geochem. Int.* **34** (11), 975–979 (1996).
- S. Lin, M. Wang, Ya. Hao, K. Zhang, Yu. Li, and D. Yang, "Synthesis, structure and thermal stability of iodine-contained sodalities  $\text{Na}_8(\text{AlSiO}_4)_6\text{Cl}_2 - x\text{I}_x$  ( $x = 0-2$ ) for  $^{129}\text{I}$  immobilization," *J. Alloys Compd.* **908**, # 164617 (2022).
- S. D. McLaughlan and D. J. Marshall, "Paramagnetic resonance of F-type centers in photochromic sodalities," *Phys. Lett.* **32A**, 343–344 (1970).
- G. B. Naumov, B. N. Ryzhenko, and I. L. Khodakovskii, *Reference Book of Thermodynamic Values (for Geologists)* (Atomizdat, Moscow, 1971) [in Russian].
- I. Norrbo, P. Gluchowski, P. Paturi, J. Sinkkonen, and M. Lastusaari, "Persistent luminescence of tenebrescent  $\text{Na}_8\text{Al}_6\text{Si}_6\text{O}_{24}(\text{Cl,S})_2$ ," *Inorg. Chem.* **54**, 7717–7724 (2015).
- L. P. Ogorodova, L. V. Melchakova, I. A. Kiseleva, and I. A. Belitsky, "Thermochemical study of natural pol-lucite," *Thermochim. Acta.* **403**, 251–256 (2003).
- L. P. Ogorodova, I. A. Kiseleva, L. V. Melchakova, M. F. Vigasina, and E. M. Spiridonov, "Enthalpy of formation of talc  $\text{Mg}_3[\text{Si}_4\text{O}_{10}](\text{OH})_2$  according to dissolution calorimetry," *Russ. J. Phys. Chem.* **85** (9), 1489–1491 (2011).
- R. C. Peterson, "The structure of hackmanite, a variety of sodalite, from Mont St-Hilaire, Quebec," *Can. Mineral.* **21**, 549–552 (1983).
- P. S. Pizani, M. C. Terrile, H. A. Farach, and C. R. Poole, "Color centers in sodalite," *Am. Mineral.* **70**, 1186–1192 (1985).
- V. Yu. Prokof'ev and N. E. Gordina, "Preparation of granulated LTA and SOD zeolites from mechanically activated mixtures of metakaolin and sodium hydroxide," *Appl. Clay Sci.* **101**, 44–51 (2014).
- T. A. Radomskaya, E. V. Kaneva, R. Yu. Shendrik, L. F. Suvorova, and N. V. Vladykin, "Sulfur-bearing sodalite—hackmanite in the alkaline pegmatites of the Inagli massif (Aldan shield): crystal chemical features, photochromism, and luminescence," *Zap. Ross. Mineral. O-va* **149** (2), 42–54 (2020).
- R. A. Robie and B. S. Hemingway, "Thermodynamic properties of minerals and related substances at 298.15 K and 1 bar (105 pascals) pressure and at higher temperatures," *U S Geol. Surv. Bull.*, No. 2131, (1995).
- A. A. Rogozhin, B. S. Gorobets, and S. V. Ryabenko, "Nature of luminescence of haloid and haloid-bearing minerals," *Mineral. Zh.* **4** (2), 45–52 (1982).
- Z. D. Sharp, G. R. Helffrich, S. R. Bohlen, and E. J. Essene, "The stability sodalite in the system  $\text{NaAlSiO}_4\text{-NaCl}$ ," *Geochim. Cosmochim. Acta* **53**, 1943–1954 (1989).
- A. Škvarlová, M. Kanuchová, L. Kozáková, E. Valušová, and M. Holub, "Preparation and characterization of ultramarine blue pigments from fly ash by using the X-ray photoelectron spectroscopy (XPS) for the determination of chemical states of sulphur in chromophores," *Micropor. Mesopor. Mater.* **284**, 283–288 (2019).
- A. N. Tarashchan, *Luminescence of Minerals* (Naukova dumka, Kiev, 1978) [in Russian].
- A. N. Tarashchan, A. N. Platonov, L. V. Bershov, and V. P. Belichenko, *Constitution and Properties of Minerals* (Naukova dumka, Kiev, 1970), Vol. 4, pp. 63–65 [in Russian].
- M. J. Taylor, D. J. Marshall, and H. Evans, "Infra-red spectra of photochromic sodalities," *J. Phys. Chem. Solids.* **32**, 2021–2026 (1971).
- E. R. Vance, D. J. Gregg, I. Karatchevseva, J. Davis, and M. Ionescu, "He and Au ion radiation damage in sodalite,  $\text{Na}_4\text{Al}_3\text{Si}_3\text{O}_{12}\text{Cl}$ ," *J. Nucl. Mater.* **453**, 307–312 (2014).
- S. C. Zilio and V. S. Bagnato, "Infrared spectra of natural sodalite," *J. Chem. Phys.* **88**, 1373–1376 (1984).

Translated by E. Kurdyukov